Title

Chlorophyll-Carotenoid Excitation Energy Transfer in High-Light-Exposed Thylakoid Membranes Investigated by Snapshot Transient Absorption Spectroscopy

Journal

Journal of the American Chemical Society, 140(38)

ISSN

0002-7863

Authors

Park, Soomin
Fischer, Alexandra L
Steen, Collin J
et al.

Publication Date

2018-09-26

DOI

10.1021/jacs.8b04844

Peer reviewed

JACS
JOURNAL OF THE AMERICAN CHEMICAL SOCIETY
Article
Cite This: J. Am. Chem. Soc. 2018, 140, 11965−11973
pubs.acs.org/JACS

Chlorophyll-Carotenoid Excitation Energy Transfer in High-Light-Exposed Thylakoid Membranes Investigated by Snapshot Transient Absorption Spectroscopy

Soomin Park,[†,‡,§,▽] Alexandra L. Fischer,[†,‡,§,▽] Collin J. Steen,[†,‡,§] Masakazu Iwai,[‡,∥] Jonathan M. Morris,[†,‡,§] Peter Jomo Walla,[§,⊥,#] Krishna K. Niyogi,[‡,∥] and Graham R. Fleming*[,†,‡,§]

[†]Department of Chemistry, University of California, Berkeley, California 94720, United States
[‡]Molecular Biophysics and Integrated Bioimaging Division, Lawrence Berkeley National Laboratory, Berkeley, California 94720, United States
[§]Kavli Energy Nanoscience Institute, Berkeley, California 94720, United States
[∥]Howard Hughes Medical Institute, Department of Plant and Microbial Biology, University of California, Berkeley, California 94720, United States
[⊥]Department for Biophysical Chemistry, Technische Universität Braunschweig, Institute for Physical and Theoretical Chemistry, Hans-Sommer-Strasse 10, 38106 Braunschweig, Germany
[#]Department of Neurobiology, Research Group Biomolecular Spectroscopy and Single Molecule Detection, Max Planck Institute for Biophysical Chemistry, Am Fassberg 11, 37077 Göttingen, Germany

Supporting Information

ABSTRACT: Nonphotochemical quenching (NPQ) provides an essential photoprotection in plants, assuring safe dissipation of excess energy as heat under high light. Although excitation energy transfer (EET) between chlorophyll (Chl) and carotenoid (Car) molecules plays an important role in NPQ, detailed information on the EET quenching mechanism under in vivo conditions, including the triggering mechanism and activation dynamics, is very limited. Here, we observed EET between the Chl Q_y state and the Car S_1 state in high-light-exposed spinach thylakoid membranes. The kinetic and spectral analyses using transient absorption (TA) spectroscopy revealed that the Car S_1 excited state absorption (ESA) signal after Chl excitation has a maximum absorption peak around 540 nm and a lifetime of ∼8 ps. Snapshot TA spectroscopy at multiple time delays allowed us to track the Car S_1 ESA signal as the thylakoid membranes were exposed to various light conditions. The obtained snapshots indicate that maximum Car S_1 ESA signal quickly rose and slightly dropped during the initial high-light exposure (<3 min) and then gradually increased with a time constant of ∼5 min after prolonged light exposure. This suggests the involvement of both rapidly activated and slowly activated mechanisms for EET quenching. 1,4-Dithiothreitol (DTT) and 3,3′-dithiobis(sulfosuccinimidyl propionate) (DTSSP) chemical treatments further support that the Car S_1 ESA signal (or the EET quenching mechanism) is primarily dependent on the accumulation of zeaxanthin and partially dependent on the reorganization of membrane proteins, perhaps due to the pH-sensing protein photosystem II subunit S.

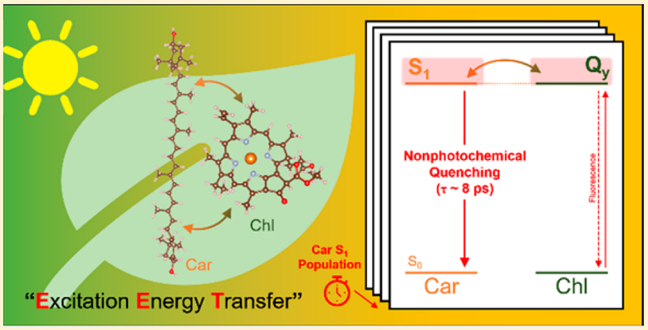

INTRODUCTION

The capacity of photosynthetic organisms to utilize the flow of excitation energy from absorbed sunlight is not unlimited. Under light-saturated conditions, the reaction center in photosystem II (PSII) closes due to lack of plastoquinones available for electron transfer.[1] As a consequence, the fluorescence lifetime (∼ns) of excited chlorophyll (Chl) in the antenna increases, which in turn increases the probability of formation of the Chl triplet state and reactive oxygen species, which can damage photosynthetic proteins.[2] Nonphotochemical quenching (NPQ) is a proxy for photoprotective thermal dissipation in which absorbed light energy is safely converted into heat.[3] NPQ is a term which encapsulates many components, termed qE, qZ, qT, and qI, which were conventionally classified based on their induction and relaxation kinetics.[3−5] Among them, energy-dependent quenching (qE) is the fastest component, and is responsible for the largest portion of overall Chl de-excitation, providing relaxation pathways for the excited Chl on a time scale of a few seconds to minutes after excess light conditions occur.[3,6]

Received: May 8, 2018
Published: September 5, 2018

DOI: 10.1021/jacs.8b04844
J. Am. Chem. Soc. 2018, 140, 11965−11973

The carotenoid (Car) pigments in PSII serve an essential role in qE.[7] In land plants, the enzymatic production of the carotenoid zeaxanthin (Zea) increases in response to high light, and Zea appears to be essential for maximum qE.[8−10] Direct involvement of Zea in Chl quenching has been suggested based on evidence of the interactions between Zea S_1 and Chl Q_y excited states.[11,12] To explain Chl-Zea energy transfer and subsequent Chl quenching, two mechanisms have been proposed: a charge-transfer (CT) quenching and excitation energy transfer (EET) quenching.[13] In the CT quenching mechanism, Chl and Zea are in close enough proximity to form a Chl-Zea heterodimer, which accepts excitation energy from the bulk Chl pool. Then, the heterodimer becomes charge-separated and forms a Zea radical cation ($Zea^{\bullet+}$) and a Chl radical anion ($Chl^{\bullet-}$).[14−17] This is followed by charge recombination which leads to energy dissipation. In the EET quenching mechanism, the excitation energy is directly transferred from the Chl Q_y state to the Zea S_1 state.[18] The direction of energy transfer is not necessarily Chl $Q_y \rightarrow$ Zea S_1, as bidirectional energy transfer, Chl $Q_y \leftrightarrow$ Zea S_1, has been shown to occur when the two state energies are similar and there is strong electronic coupling between them.[13,19−22] After energy transfer, the Zea S_1 state rapidly relaxes to the ground state with a lifetime of ∼9 ps.[18,23−25] Other carotenoids, such as lutein (Lut), have also been considered as direct quenchers in CT and EET quenching mechanisms.[7,26,27] Although it has been speculated that both quenching mechanisms contribute to overall qE, the specific details of the quenching sites, triggering factors, activation time courses, and relative contributions of individual mechanisms are not well understood.

Recently, we reported the use of snapshot transient absorption (TA) spectroscopy to gather quantitative and dynamic information on the $Zea^{\bullet+}$-mediated CT quenching mechanism in high-light-exposed spinach thylakoid membranes.[17] Those experiments focused on one wavelength (1000 nm) and time delay (20 ps), and allowed us to collect the $Zea^{\bullet+}$ excited state absorption (ESA) signal within 10 s windows over the course of high-light exposure. The $Zea^{\bullet+}$ ESA signal reaches maximum intensity at the beginning (≤2 min) of high-light exposure, which suggests that $Zea^{\bullet+}$ formation is closely related to early qE. The evolution of the $Zea^{\bullet+}$ signal correlated well with the lumenal $[H^+]$ and the rate of Chl fluorescence quenching. In addition, a cross-linking assay[28] arresting rearrangement of the pH-sensing PSII subunit S (PsbS) protein completely removed $Zea^{\bullet+}$ signals, and suggested that the CT quenching mechanism was triggered by a ΔpH → messenger protein(s) pathway.[6,29]

Here, to investigate a Chl-Car EET quenching mechanism in thylakoid membranes during exposure to high-light, we have modified our above-mentioned snapshot TA technique to probe at 540 nm where the maximum Car S_1-S_N absorption is observed. Increased population of the Car S_1 state after Chl excitation (650 nm) should provide evidence for the EET quenching mechanism.[21,23,30] Combining the new data with fluorescence lifetime snapshot data and our previous $Zea^{\bullet+}$ snapshot data,[17] we can provide a broader picture of the EET and CT quenching mechanisms.

EXPERIMENTAL METHODS

Isolation of Thylakoid Membranes. Fresh spinach leaves were purchased the day before the measurements and stored in the dark at 4 °C overnight. The spinach leaves used in the experiment were grown in northern California and harvested in early spring (February to March). Isolation of crude thylakoid membranes was performed in a dark cold room (4 °C), following the protocol reported by Gilmore et al.[31] The final concentrations of all thylakoid samples were adjusted to 100 μg Chl/mL using reaction buffer before measurement. The reaction buffer at pH 8 contained 30 mM ascorbic acid, 0.5 mM ATP, and 50 μM methyl viologen. The working concentrations of DTSSP and DTT were 3 and 2 mM, respectively.

Pump−Probe Spectroscopy for TA Measurements. A description of the pump−probe transient absorption spectroscopy setup used in this study can be found in previous literature.[14−17] Briefly, the experiments were performed using a Ti:sapphire regenerative amplifier (Coherent, RegA 9050) seeded by a Ti:sapphire oscillator (Coherent, MIRA Seed), generating an 800 nm pulse with a repetition rate of 250 kHz. The beam was split to generate the pump and probe beams. For the probe, the beam was focused on a 1 mm sapphire crystal to produce a visible continuum, and a 700 nm short pass filter was placed after continuum generation. For the pump, another beam pumped an optical parametric amplifier (Coherent, OPA 9450). The OPA was tuned to generate a 20 nJ/pulse centered at 650 nm for the Chl b Q_y transition which yielded higher signal-to-noise ratio than 680 nm. The fwhm of pump pulses was 50 fs. The pump and probe were overlapped at the sample at the magic-angle (54.7°) polarization. The diameters of the pump and probe at the sample position were 150 and 65 μm, respectively. The cross-correlation time between the pump pulse and probe pulse was found to be ∼120 fs. After the sample, a second polarization filter set to the probe polarization and a 658 ± 26 nm notch filter were placed to minimize pump scattering and ensure a clean probe signal. After passing through a monochromator (Acton Research Corp., SpectraPro 300i), the signal was detected by using a Si-biased photodiode (Thorlabs, DET10A) which was connected to a lock-in amplifier (Stanford Research, SR830). The lock-in amplifier was synchronized with a chopper positioned in the pump beam path. An actinic light with a heat absorbing filter (KG1) was set to an intensity of 850 μmol photons·m^{-2}·s^{-1} at the sample position. For collecting snapshot TA data at fixed time delays (1 and 40 ps) and wavelength (540 nm), a pump and probe shutter was controlled to open for 10 s at intervals ranging from 30 s to 1 min throughout the high-light-exposure sequence. The sample cell was translocated continuously to prevent sample damage. The path length of the cuvette was 1 mm.

Fluorescence Lifetime Snapshot. Fluorescence decay snapshots were recorded with a home-built time-correlated single photon counting (TCSPC) apparatus described previously.[32−34] First, 840 nm output pulses generated by Ti:sapphire oscillator (Coherent, Mira 900f, 76 MHz) were frequency-doubled using a beta barium borate (BBO) crystal. The resultant 420 nm pulses correspond to the Soret band absorption of Chl a. Before the sample, the beam was split by a beam splitter, so that a portion was directed to a photodiode providing SYNC for the TCSPC card (Becker-Hickl, SPC-630 and SPC-850). The remainder of the beam was sent to excite the sample and was intermittently blocked by a shutter controlled by a LabVIEW program. The excitation laser power was set to 1.6 mW (≅1650 μmol photons·m^{-2}·s^{-1}) at the sample, which is enough to close reaction centers.[35] The sample was intermittently exposed to an actinic light (Schott, KL1500) with an intensity of 850 μmol photons·m^{-2}·s^{-1}, also controlled by a shutter and LabVIEW program. After the sample, a monochromator set to 680 nm and a MCP PMT detector (Hamamatsu, R3809U) were placed for fluorescence detection. The fluorescence decay curves were measured at intervals varying from every 10 s to every 30 s. In each measurement, the sample was exposed to the laser for one second, divided up into five steps of 0.2 s. The step with the longest fluorescence lifetime was selected in data processing to ensure that the PSII reaction centers were closed.[34] Each fluorescence decay curve was fit to a sum of three exponential decay components (Picoquant, Fluofit Pro-4.6). Following data fitting, the amplitude-weighted average lifetime ($\tau_{average}$) and NPQ_τ values were calculated using the following equations:[17,33,34]

DOI: 10.1021/jacs.8b04844
J. Am. Chem. Soc. 2018, 140, 11965−11973

$$\tau_{avg} = \frac{\sum_i A_i \tau_i}{\sum_i A_i} \quad (1)$$

where A_i and τ_i are the amplitudes and the fluorescence lifetime components, respectively.

$$NPQ_\tau = \frac{\tau_{avg,dark} - \tau_{avg,light}}{\tau_{avg,light}} \quad (2)$$

where $\tau_{avg,dark}$ is the average of three lifetimes measured during the initial dark period.

RESULTS

TA Kinetic Profile and Spectrum of Car S_1 ESA. Figure 1a shows the TA kinetic profiles of high-light- and dark-exposed thylakoid membranes probed at 540 nm. At wavelengths longer than 520 nm, there is a considerable amount of Chl ESA signal detected in addition to Car S_1-S_N absorption.[36] As Chl Q_y excited states depopulate via quenching or another de-excitation pathway, the intensity of the ESA signal corresponding to Chl Q_y decreases significantly, which explains why high-light-exposed samples have an overall lower level of ESA signal compared to dark-adapted samples (Figure 1a). Correspondingly, the Car S_1-S_N transition becomes the more dominant signal at shorter time delays under high-light conditions. We found that the two TA kinetic profiles are kinetically indistinguishable at longer time delays (≥40 ps) at which the Car S_1 ESA contribution should be negligible.[18,21] To account for the significant decrease in Chl ESA and clearly compare TA kinetic profiles, we scaled the profile of the dark-exposed sample to match that of the high-light-exposed profile based on signals at around 40 ps time delay. Figure 1b shows that the high-light-exposed profile and scaled dark-exposed profile overlap well at time delays greater than 40 ps.

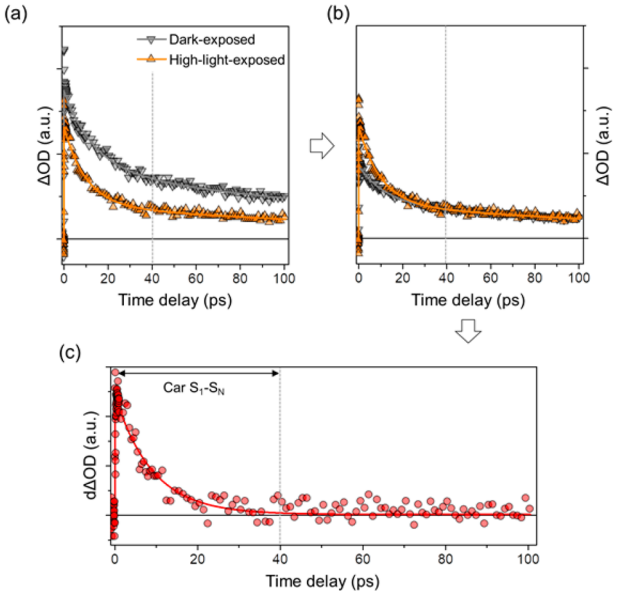

Figure 1. (a) TA kinetic profiles for spinach thylakoid membranes under dark (gray, down triangle) and high-light (orange, up triangle) conditions. The samples were excited and probed at 650 and 540 nm, respectively. (b) Scaled TA kinetic trace obtained by matching the dark-exposed thylakoids (gray, down triangle) to the respective trace measured under high-light conditions (orange, up triangle) at a time delay of 40 ps. (c) Difference between high-light and scaled dark-exposed kinetic profiles. For the high-light condition, thylakoids were continuously exposed to actinic light at 850 μmol photons·m^{-2}·s^{-1}.

Figure 1c shows the difference between the high-light- and dark-exposed (scaled) profiles. The difference profile fits well to a single exponential decay, with a lifetime of 7.81 ps (±0.83 ps). This value agrees with the literature values of the S_1 lifetime of Zea, which range from 7 to 11 ps.[18,23,24] In this fit, there was no resolvable rise time within the time resolution (~120 fs) of our TA setup.[18,21] If we consider the difference decay profile as the excitation energy population in the Car S_1 state, a lack of resolvable rise time indicates near instantaneous excitation equilibrium near Chl-Car EET quenching sites. One possible scenario is that the mixing of Chl Q_y and Car S_1 states is reinforced by increased electronic coupling after high-light exposure, which eventually results in instantaneous excitation equilibrium via bidirectional energy transfer between Chl-Car at EET quenching sites. Such bidirectional Chl-Car EET was observed experimentally by Kennis,[13] Walla,[19−22] and co-workers.

To determine the origin of the signal in Figure 1c, we performed a global analysis on the TA kinetic profiles of high-light-exposed thylakoid samples. Through global analysis, it was deduced that at least three lifetime components (τ_1 = 7.81 ps, τ_2 = 28.2 ps, and τ_3 = 160 ps) are required for fitting the ESA signals in the wavelength range of 530−620 nm (Figure S1). From the TA kinetic profile at 620 nm, the two longest lifetime components (τ_2 = 28.2 ps and τ_3 = 160 ps) mainly represent the contribution of Chl ESA. As shown in Figure 2, the lifetime component of 7.81 ps with maximum absorption amplitude at 540 nm strongly resembles the S_1-S_N absorption spectrum of Zea in methanol from Polívka et al., which features an asymmetric peak centered at 555 nm.[24,37] The peak in Figure 2 is slightly blue-shifted (~15 nm) from the spectra reported previously,[24,37] likely due to differences between solvent vs protein environments. A similar magnitude of blue-shift in the spinach thylakoid membrane environment has also been observed in previous studies.[18,21] Considering its lifetime (~8 ps) and spectrum, it seems likely that the observed ESA signal is from a Car S_1-S_N transition, and the Car is presumably Zea.

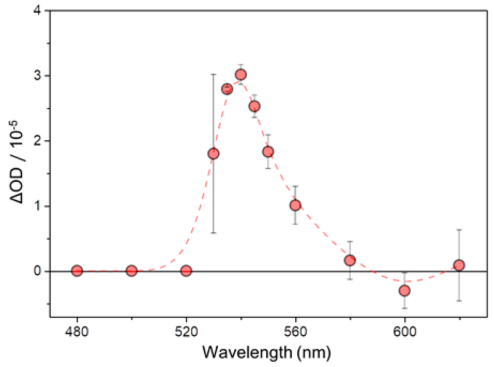

Figure 2. The 7.81 ps decay component-associated spectrum obtained by global analysis of the decay profiles of excited state absorption signals measured on high-light-exposed thylakoids. The decay profile at each wavelength is presented in Figure S1. Data are presented as the fit parameters ± SE. Dashed line represents a b-spline interpolation among the data points.

Kinetic Analysis. To further confirm the origin of the observed signal, we explored possible kinetic pathways that

DOI: 10.1021/jacs.8b04844
J. Am. Chem. Soc. 2018, 140, 11965−11973

would lead to the dynamics observed in Figure 1c. Considering that the Chl fluorescence lifetime of the thylakoid membrane is in the range of 0.35−1.47 ns (Figure 5a), it is probable that Chl*−Chl* annihilation is the dominant factor in determining the rate of Chl* de-excitation and the excitation diffusion length, which results in a shortened Chl ESA signal lifetime ($\tau_{average}$ < 0.1 ns) in our TA measurement. The signal decay difference between dark- and high-light-exposed samples was negligible at 620 and 680 nm where Chl ESA and ground state bleaching signals dominate, respectively (Figure S2). If the high-light exposure were to cause variations in Chl excitation energy dynamics beyond turning on quenching mechanisms (e.g., Chl*−Chl* annihilation), a significant change should appear at 620 and 680 nm. Therefore, it is reasonable to assume that Chl*−Chl* annihilation is consistent during the transition from dark to high light.

Before continuing our analysis, we note that the relative time scales of excitation transport and/or trapping in the photosystem II antenna system would suggest that observing states with lifetimes as short as 8 ps would be very difficult, if not impossible, due to the extremely low steady-state concentration of the short-lived species if the formation time is several hundred picoseconds. However, the presence of Chl*−Chl* annihilation in the TA measurement restricts the diffusion length of excitations in the antenna and enables the direct observation of short-lived intermediates. Valkunas and coworkers estimated a rapid annihilation rate of (16 ps)$^{-1}$ per light-harvesting complex II (LHCII) trimer for extended aggregates.[38] If we assume that annihilation in thylakoid membranes occurs on a much faster time scale than the excitation migration time through LHCII to an immobilized trap, the presence of the annihilation process will reduce the excitation diffusion length. A key feature in our data is the lack of an observable rise time in the excited signal at 540 nm, in contrast to our data at 1000 nm.[14,17] Below we show that this difference arises from the differing lifetimes of the two quenching species.

The dynamics of the Car S_1 state population was investigated using a linear chain model in which instantaneous excitation equilibrium between a subset of Chl and Car was assumed (Figure 3a). To model how Chl*−Chl* annihilation influences the Car S_1 population after Chl excitation, we divided the total Chl population into two groups. The ***Y*** group contains Chl molecules that are close enough to a Car molecule in a configuration consistent with downhill energy transfer such that EET would be very rapid, while the ***X*** group contains all other Chl molecules that are far enough away from a Car molecule in a quenching configuration such that EET would be significantly slower. By varying the initial populations of the ***X*** and ***Y*** groups that are excited, which are depicted as the relative percentages of Chl excitations in Figure 3b, we can observe changes in the dynamics of the excited Car S_1 state. Figure 3b suggests that only Chl that are excited very close to Car molecules will populate the Car S_1 state we observe. Increasing the proportion of Chl excited near a Car (***Y***) to just 10% of the excited population in the bulk Chl pool (***X*** group) removes the rise component and results in a decay profile of the Car S_1 population that is well overlapped with the experimentally observed difference decay profile (Figure 3b). The absence of a rise component in the Car S_1 kinetic profile differs from the previously observed $Zea^{\bullet+}$ kinetic profiles, which are fitted with rise and decay components.[14−16] This difference can be attributed to the fact that a slower de-

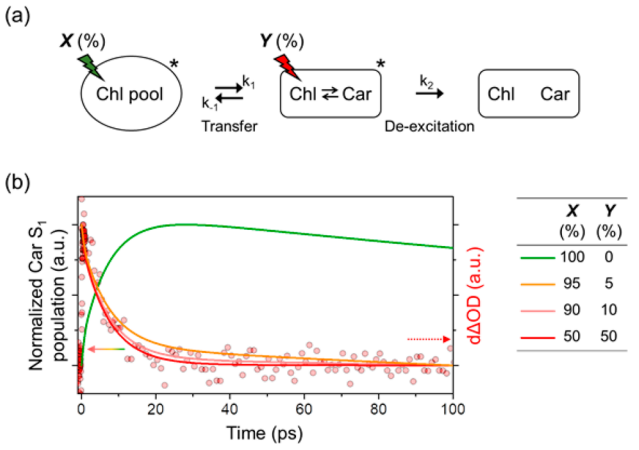

Figure 3. (a) Kinetic scheme for the EET quenching mechanism in high-light-exposed thylakoid membranes. The coupled Chl Q_y-Car S_1 state is regarded as an individual state which signifies a near instantaneous excitation equilibrium via bidirectional Chl↔Car energy transfer or a very rapid (≤120 fs) buildup of population in Car S_1 state at quenching sites. Relative percentages of Chl excitations between Chl pool and a Chl adjacent to Car are denoted as ***X*** and ***Y***, respectively. The rate constants k_1 and k_{-1} were assumed to be (350 ps)$^{-1}$ based on our bulk Chl fluorescence lifetime in the quenched state (Figure 5a). k_2 is (8 ps)$^{-1}$ based on the lifetime of the Zea S_1 state.[16,21,22] (b) Dynamics of the Car S_1 state population calculated with various initial excitation populations of the bulk Chl pool vs Chl close to Car. The solid curves represent the simulated dynamics. The difference TA kinetic data points (red dots) from Figure 1c are also displayed.

excitation rate (≤2.5 × 10^{10} s^{-1}) of the CT state allows for the observation of an increase in the $Zea^{\bullet+}$ population after Chl excitation (Figure S3).

We also considered a second possibility: that rapid membrane restructuring occurs in high-light conditions, producing small isolated clusters of LHCIIs each containing a quenching site. This, rather implausible, scenario would explain the lack of rise time for the Car S_1 signal, though not the existence of a rise time for the $Zea^{\bullet+}$ signal.[14−16] It is also difficult to see how this would provide effective protection to the reaction center in the presence of excess light. Nor does it seem likely that such a mechanism would be rapidly reversible or provide such clear correspondence between the absorption and fluorescence data which will be presented in the following text. Accordingly, we did not pursue this model further.

Snapshot TA Spectroscopy. Using the previously described method for extracting the Car S_1 ESA signal from Chl ESA at 540 nm, we performed snapshot TA measurements at two different time delays after the excitation pulse. The Car S_1 ESA signal has a decay constant of less than 10 ps, while the Chl ESA signal decays on a much longer time scale.[18] Therefore, the TA signal was measured at 40 ps to account for the overall decrease in Chl ESA as thylakoids were exposed to high light. The Car S_1 ESA signal has disappeared by this time delay (Figure 1c). Therefore, to measure Car S_1 ESA at 540 nm, the signal is measured at a delay time of 1 ps, then scaled using the 40 ps signal to account for the underlying decrease in Chl a ESA signal:

DOI: 10.1021/jacs.8b04844
J. Am. Chem. Soc. 2018, 140, 11965−11973

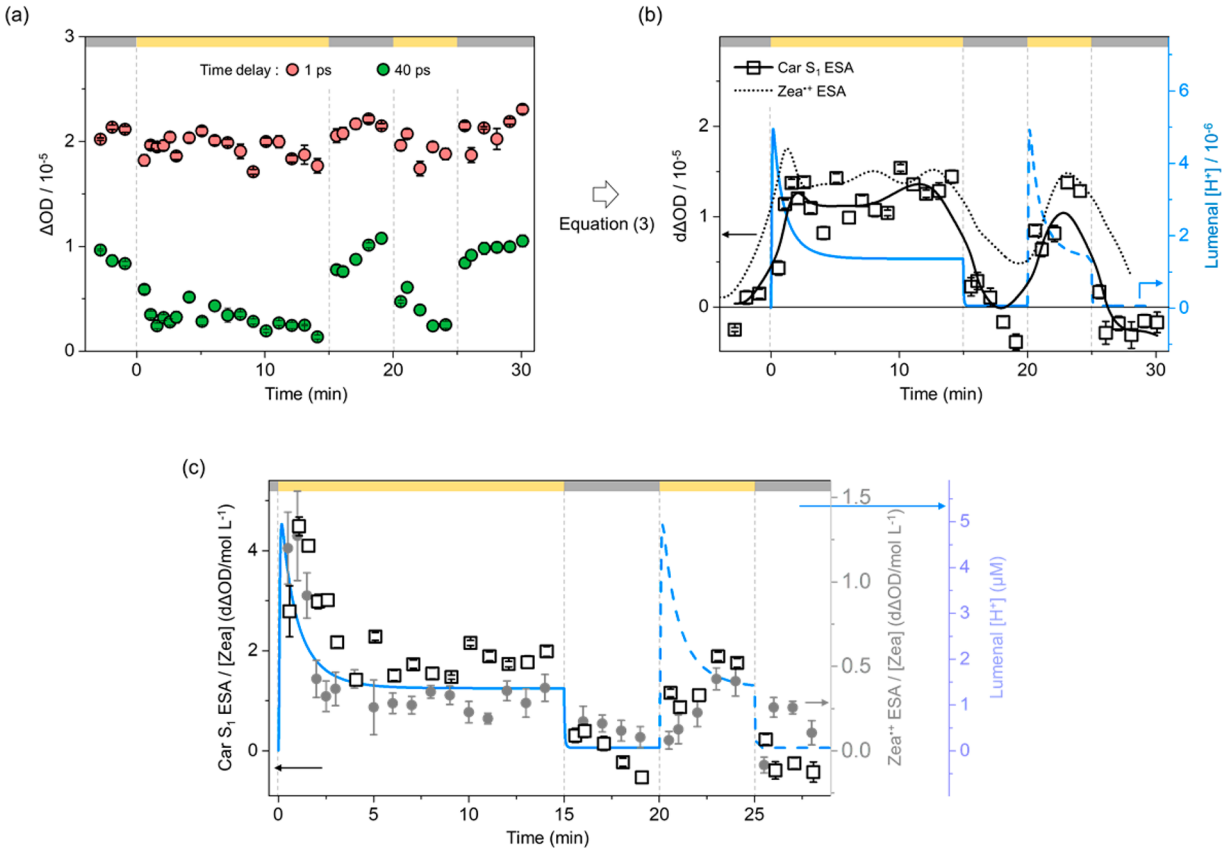

Figure 4. (a) Snapshot TA data obtained at 1 ps (red) and 40 ps (green) after Chl excitation. The vertical lines (gray, dashed) and bars at the top of the figures indicate the time sequence of actinic light on (yellow) and off (dark gray). (b) Difference (high-light-exposed minus dark-exposed) snapshot TA data at 1 ps (black, squares) with the zero line representing the average signal during the initial dark period. See eq 3 in the text for the calculation of the difference snapshot TA data (dΔOD). The solid black line is a smoothed line from the data points corresponding to Car S_1 ESA. The smoothed line for $Zea^{\bullet+}$ absorption (dotted line) from high-light-exposed spinach thylakoids is also displayed.[17] The calculated lumenal $[H^+]$ (blue line) in response to high-light/dark exposures is based on the kinetic model described by Zaks et al.[6,29] Note that there is considerable uncertainty in the lumenal $[H^+]$ during the second high-light exposure period as the model was devised for completely dark-adapted systems. (c) Evolution of normalized Car S_1 absorption (Car S_1 ESA/[Zea]) (black squares) and normalized $Zea^{\bullet+}$ absorption ($Zea^{\bullet+}$ ESA/[Zea]) (gray circles). [Zea] was determined by time-resolved HPLC measurements (Figure S5). All data are presented as the mean ± SE (n = 5).

$$\mathrm{d}\Delta\mathrm{OD}_{\mathrm{Car}S_1}(t) = \Delta\mathrm{OD}_{\mathrm{at1ps}}(t) - \Delta\mathrm{OD}_{\mathrm{at1ps}}(\mathrm{dark}) \times \left(\frac{\Delta\mathrm{OD}_{\mathrm{at40ps}}(t)}{\Delta\mathrm{OD}_{\mathrm{at40ps}}(\mathrm{dark})} \right) \quad (3)$$

where $\Delta\mathrm{OD}_{\mathrm{at1ps}}(t)$ and $\Delta\mathrm{OD}_{\mathrm{at40ps}}(t)$ represent the snapshot TA signal measured at time delays of 1 and 40 ps, respectively. ΔOD (dark) is the average of TA signals measured during the initial dark period. The dΔOD spectrum presented in Figure S4, reconstructed by the same scaling and subtraction at various wavelengths, shows a distinct peak centered at 540 nm, which proves the validity of the above-mentioned method (eq 3) for extracting dΔOD values corresponding to Car S_1 ESA.

Figure 4a shows individual snapshot TA results measured at 1 and 40 ps during a time sequence of the actinic light turning on and off. Each data point in the 1 ps trace is then scaled using the data point of the corresponding light exposure time in the 40 ps trace, which gives the result shown in Figure 4b, overlaid with data from the $Zea^{\bullet+}$ snapshot TA data of Park et al.[17] Much like the $Zea^{\bullet+}$ signal, the Car S_1 ESA signal appears very rapidly (<3 min) after the actinic light is turned on, well within the time scale of the qE response. Considering the fact that Zea accumulates exponentially with a rise time of 2−3 min,[17] it seems surprising that the amount of Car S_1 ESA signal indicative of Chl-Zea EET quenching is substantial in the early stages (≲3 min) of qE. This difference in time scale may result from ΔpH or ΔpH-triggered mechanisms,[29] such as a structural change in LHC proteins, which may enhance the appearance of the Car S_1 ESA signal in early qE. If this is so, during the first few minutes of high-light exposure, the amount of EET quenching may not be significantly limited by the concentration of Zea. In this context, we note that in the coarse-grained model of qE in the grana membrane developed by Bennett et al.,[39] wild-type levels of qE can be achieved with only 12−15% of potential LHCII quenching sites active as quenchers. Notably, both Car S_1 and $Zea^{\bullet+}$ ESA signals are well-correlated with ΔpH calculated from the model developed by Zaks et al. at early qE (Figure 4c), suggesting the important role of ΔpH or ΔpH-triggered mechanisms.

After the initial rapid response, the Car S_1 ESA signal appears to drop, then increases more slowly, perhaps implying the existence of both rapidly activated and slowly activated mechanisms. Two quenching time scales were previously observed by Dall'Osto et al. in *Arabidposis thaliana* plants lacking minor complexes.[40] Interestingly, the Car S_1 ESA signal disappears very rapidly (≲1 min) after turning the actinic light off, much faster than the $Zea^{\bullet+}$ signal, which does not fully disappear even after the actinic light has been turned off for 5

DOI: 10.1021/jacs.8b04844
J. Am. Chem. Soc. 2018, 140, 11965−11973

min.[17] The rapid disappearance of Car S_1 ESA signal in response to dark exposure suggests that the EET quenching mechanism plays a central role in rapidly reversible qE quenching, which is known to improve plant fitness under fluctuating light conditions.[41,42] In addition, it is conceivable that the CT and EET mechanisms involve different protein/carotenoid conformations with one able to relax more quickly than the other.[43]

Under in vivo conditions, for sufficiently strong Chl−Car coupling, the average lifetime of overall excited Chl could significantly decrease as coupled Chl−Car molecules form in grana membranes during high-light exposure.[12,36] In order to compare the Car S_1 ESA data with data on the overall Chl fluorescence quenching, changes in the Chl fluorescence lifetime of the same thylakoid samples used for snapshot TA were monitored during high-light exposure using fluorescence lifetime snapshot spectroscopy.[32−34] Examining the Chl fluorescence decay and corresponding lifetime value ($\tau_{average}$) at each time point allows for the assessment of Chl* quenching independent of Chl concentration, Chl*-Chl* annihilation, or photobleaching. Figure 5a and b presents $\tau_{average}$ and calculated NPQ parameters (NPQτ), respectively. NPQτ values are closely related to the conventional NPQ parameter (see Experimental Methods).[17,33] Notably, the appearance time of the Car S_1 ESA presented in Figure 4b coincides with the Chl* quenching indicated by NPQτ (Figure 5b).

Chemical Treatments. To examine Car S_1 ESA in thylakoids without accumulated Zea, samples were treated with 1,4-dithiothreitol (DTT) to inhibit violaxanthin de-epoxidase (VDE) activity.[44,45] VDE is a thylakoid lumen protein responsible for the accumulation of Zea by de-epoxidizing violaxanthin in response to lumen acidification.[8,9] Time-resolved high-performance liquid chromatography revealed that the accumulation of Zea is not noticeable under DTT-treated conditions (Figure S5). The DTT-treated thylakoid showed a substantially lowered NPQτ value compared to the untreated sample (Figure 5b). As shown in Figure 5c, the snapshot TA data of the DTT-treated thylakoid showed a transient spike in the Car S_1 ESA signal in the first 2 min of high-light exposure. However, after the spike, there was no signal higher than that of the initial dark-exposed state, suggesting that Zea accumulation is necessary to sustain a Chl−Car EET quenching process. This observation, together with its lifetime of ∼8 ps, strongly suggests that the Zea S_1 state is directly involved in EET quenching of excited Chl.

Slightly negative signals were observed with DTT after 10 min of high-light exposure. We speculate that the process of high-light exposure under the condition that few quenchers are available can slightly alter Chl ESA dynamics or Chl*−Chl* annihilation (Figure S6) which likely originates from a structural difference in dark- and light-exposed grana membranes and/or the early onset of other quenching processes. The DTT treatment may also alter the way the membrane responds to high light and returns to low light.

Cross-linking using 3,3′-dithiobis(sulfosuccinimidyl propionate) (DTSSP) is suggested to stop PsbS-controlled conformational changes of the thylakoid membrane, resulting in behavior similar to the *npq4 Arabidposis thaliana* mutant.[17,28,46] As reported previously, DTSSP-treated and *npq4* thylakoids do not show any $Zea^{\bullet+}$ TA signal, consistent with the idea that the interactions of active PsbS are essential for $Zea^{\bullet+}$ formation that is indicative of CT quenching.[14,17] Interestingly, DTSSP-treated thylakoids showed a 50% lower amount of Car S_1 ESA signal compared to the untreated sample (Figure 5c). In addition, the signal was largely unchanged during subsequent changes in actinic light intensity. This result suggests that deactivated PsbS does not completely remove EET quenching induction, and its activation allows for a larger quantity of EET quenching and improves the reversibility.[33,47]

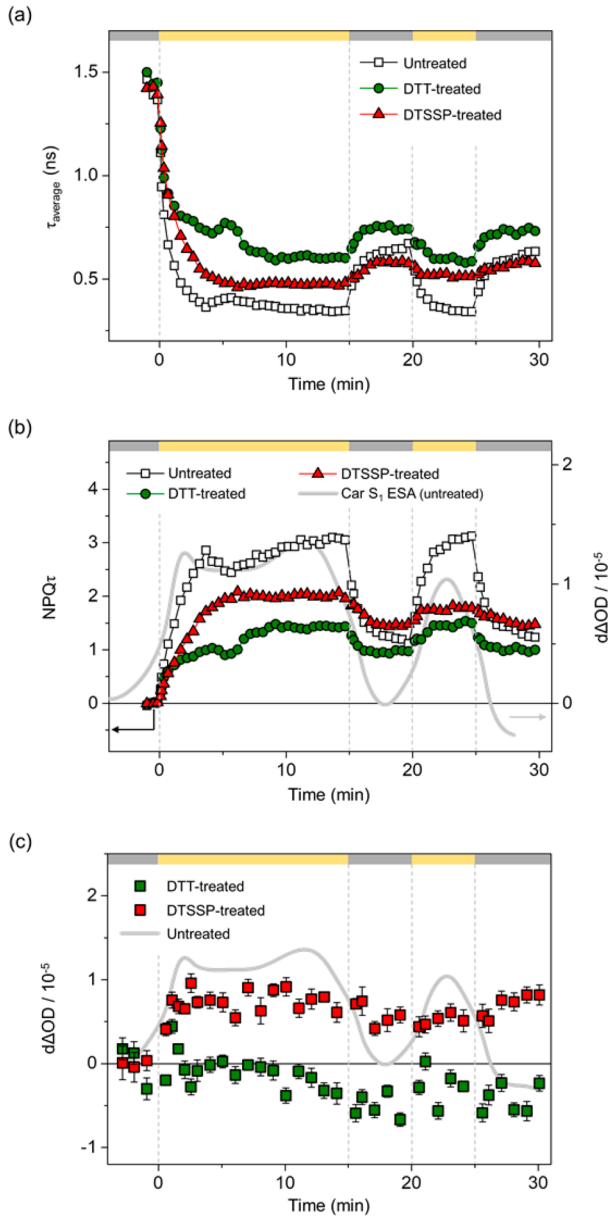

Figure 5. Fluorescence lifetime snapshot results presented as (a) average chlorophyll fluorescence lifetimes ($\tau_{average}$) and (b) calculated NPQτ values of untreated (white squares), DTT (green circles)- and DTSSP (red triangles)-treated thylakoids in response to high-light/dark exposure. The vertical lines (gray, dashed) and bars at the top of the figures indicate the time sequence of actinic light on (yellow) and off (dark gray). See Experimental Methods for further discussion of $\tau_{average}$ and NPQτ values. The Car S_1 ESA signal of the untreated sample is displayed as a smoothed trajectory (gray curve). (c) Difference (high-light-exposed minus dark-exposed) TA snapshot results of DTSSP (red)- and DTT (green)-treated thylakoid membranes at 540 nm and 1 ps delay time. The zero line represents the averaged signal from the initial dark period. See eq 3 in the text for the calculation of the difference snapshot TA data (dΔOD). Data are presented as the mean ± SE (n = 5).

DOI: 10.1021/jacs.8b04844
J. Am. Chem. Soc. 2018, 140, 11965−11973

DISCUSSION

Recently, Croce and co-workers reported that intense Chl*−Chl* annihilation and a higher excited state of Chl *a* within isolated LHCII produced a (Chl *a*-Lut)* byproduct (referred to as **Q**) which has a ESA peak at around 535 nm.[48] We closely examined the reported **Q** ESA and compared it to our Car S_1 ESA data in case the high-light exposure significantly increases the extent of Chl*−Chl* annihilation, which would seem unlikely. The Car S_1 ESA signals observed in this study have decay time constants of ∼8 ps, and are very small by 20 ps after Chl excitation (650 nm). Our Car S_1 ESA kinetics remained unchanged when measured under various pump intensities. In contrast, the majority of the **Q** ESA signal remains after 20 ps as the species appears to be relatively long-lived or slow-formed. According to the species-associated difference spectrum of **Q**, the measured **Q** state is populated with a time constant of several picoseconds. However, the rise time component of Car S_1 ESA signal was not resolvable with the time resolution (≅120 fs) of our TA setup. Consequently, the kinetics of the Car S_1 ESA signals appear quite distinct from that of **Q** and exhibit a fast decay time constant very similar to the values for xanthophyll S_1 lifetimes obtained in annihilation-free conditions in dilute solution.[23−25] The signals in both this work and our previous study of CT quenching are observable because of the restricted diffusion length of excitation through moderate excitation annihilation. It is important to ask, then, if the intrinsic rate of CT or EET quenching is accurately obtained from the data reported here and in previous literature.[14−18,21] As the simple model calculation in Figure 3 shows, for quite small (∼10%) and either direct or very rapid (≤120 fs) population of the quencher state, within our experimental error, the same decay time (≅8 ps) is observed for Zea S_1.[23−25] The CT ($Chl^{\bullet-}$−$Zea^{\bullet+}$) states in thylakoid membranes have been observed to have longer decay times (40−150 ps)[14,17] which could be influenced by Chl-Zea separation and the surrounding protein environment. We therefore consider that the time scales of the decay of the two trap states are the ones that should be used in quantitative models of qE such as that of Bennett et al.[39] Incorporation of Chl*−Chl* annihilation into such a model should enable a quantitative estimate of the relative importance of EET and CT mechanisms.

The thylakoid membrane contains several carotenoids in addition to the violaxanthin−antheraxanthin−zeaxanthin set. Of these, Lut is a key component of LHCII and has also been proposed as a quencher of excited Chl.[7] Spectroscopic studies on isolated LHCs[27] and calculations of excitation quenching in LHCII focused on Lut coupled to $Chla_{610}$−$Chla_{611}$−$Chla_{612}$ domain[49,50] have argued that Chl → Lut excitation energy transfer is a possible quenching pathway. In our view, several lines of evidence suggest that Zea is the major quencher in our study reported here. The lifetime of the Car S_1 ESA signal observed is ∼8 ps. As discussed above, this value coincides with literature values for the S_1 lifetime of Zea, which range from 7 to 11 ps.[18,23,24] On the other hand, Lut has a S_1 lifetime of ∼14 ps,[24] which is significantly different from our experimental observation. More importantly, DTT-treated thylakoids showed no Car S_1 ESA signal, strongly suggesting that the Zea S_1 state is predominantly responsible for EET quenching in high-light-exposed spinach thylakoids. The extent to which isolated pigment−protein complexes provide an accurate guide for the natural system is not clear. There may well be structural and conformational differences between pigment−protein complexes within isolated LHCII and intact thylakoid membranes. Indeed, significant differences are seen in Chl fluorescence lifetimes of detergent-solubilized LHCII (>3 ns),[51] aggregated LHCII crystals (0.2−1.5 ns),[52] and thylakoids (0.35−1.47 ns; this study). It has been reported that the presence of Lut can recover the wild type phenotype in the absence of Zea, indicating that Lut can replace Zea as a quencher.[26,32] However, on a per-molecule basis, Zea in intact leaves is estimated to be 10 times more effective in overall Chl* quenching than Lut,[32] consistent with the snapshot TA data in this study. Nonetheless, we cannot completely rule out the possibility that accumulated Zea indirectly facilitates Lut S_1-mediated EET quenching and that both Zea S_1 and Lut S_1 states are involved in such quenching.[27] Future snapshot TA studies of various mutants containing different levels of Zea and Lut (e.g., *npq1*, *szl1npq1*, and *lut2*) should greatly aid in the investigation of Zea S_1- and Lut S_1-mediated EET quenching in the native state.

In our previous work,[17] we found that inhibiting the activity of PsbS by DTSSP removed the $Zea^{\bullet+}$ signal, and an increased $Zea^{\bullet+}$ signal was observed when a higher concentration of Zea was available for excited Chl quenching as a result of the VDE action. Somewhat similarly, Zea accumulation is necessary for the Car S_1 ESA signal, though activated PsbS further increases the Car S_1 ESA signal. This suggests that both Zea and PsbS are required to achieve maximum EET and CT quenching. However, the degree to which each signal relies on each component differs significantly, as evidenced by their differing responses to chemical treatments (Figure 5c). For example, the $Zea^{\bullet+}$ ESA signal was eliminated with the addition of PsbS-inhibiting DTSSP.[17] Meanwhile, the Car S_1 ESA signal was considerably less affected by the DTSSP treatment, indicating that activation of EET quenching via a PsbS-triggered pathway is not the only activation mechanism. It is also noteworthy that the $Zea^{\bullet+}$ ESA signal appeared very quickly after high-light exposure (≤30 s),[17] while the Car S_1 ESA signal appears more slowly after high-light exposure (≤1 min), suggesting differing dependences on a fast-acting PsbS pathway.

The apparently biphasic activation of EET quenching further implies the existence of two different triggering pathways, which are activated on different time scales (Figure S7). In this scenario, the fast pathway seems to be mainly directed by activated PsbS in response to ΔpH. The activation of this pathway is not significantly limited by the concentration of Zea, which is supported by the snapshots of DTT-treated samples showing a positive Car S_1 ESA signal during the early period of high-light exposure (≤2 min) (Figure 5c). In contrast, the slower activation pathway seems to be primarily dependent on the accumulation of Zea. Although active PsbS/membrane reorganization may be less influential in the activation of EET quenching, PsbS likely still plays an important role in dark recovery, as shown in Figure 5c where the addition of DTSSP removed much of the reversibility of the Car S_1 ESA signal. Overall, we speculate that the operation of these two triggering pathways enables the rapid establishment and sustained operation of the EET quenching mechanism, emphasizing its importance in qE (Scheme 1).

A study on a cyanobacterial LHC protein showed that switching into the quenched state can be achieved by very subtle changes in pigment−protein or pigment−pigment interactions.[43] In this context, it is probable that these different

DOI: 10.1021/jacs.8b04844
J. Am. Chem. Soc. 2018, 140, 11965−11973

Scheme 1. Proposed Scheme for the Triggering System of the EET and CT Quenching Mechanisms for qE[a]

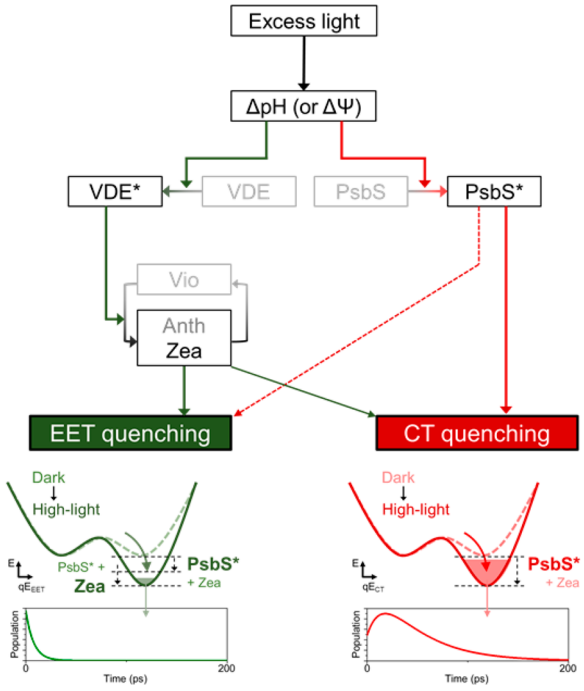

[a]Regarding the involvement of PsbS and Zea, essential steps are denoted by solid arrows, and nonessential but influential steps are denoted by the dashed arrow. VDE* and PsbS* represent activated proteins by ΔpH and protonation, respectively. In the very initial stages of high-light exposure, CT quenching appears to depend on the small pool of Zea (or Anth) that is present in the dark.[17]

states include different Chl−Car distances, excited state couplings, and relative site energies, which could make certain quenching pathways viable in the intact system but not in isolated complexes, or vice versa. The picture that emerges from these and other recent studies is of a highly flexible control system capable of being switched by small structural changes between at least two quenching pathways: EET and CT. By biasing the inherent structural fluctuations of light harvesting pigment−protein complexes through pigment exchange, protein−protein interactions, and gradients of protons or ions, a system capable of rapid (seconds to minutes) responses to light level changes protects green plants from photo-oxidative damage.

■ ASSOCIATED CONTENT

Supporting Information

The Supporting Information is available free of charge on the ACS Publications website at DOI: 10.1021/jacs.8b04844.

Results of TA profiles/spectrum, TA kinetic profiles of DTT-treated sample, kinetic scheme/simulation for CT quenching mechanism, time-resolved HPLC data, and snapshot TA data with curve fit (PDF)

■ AUTHOR INFORMATION

Corresponding Author

*grfleming@lbl.gov

ORCID

Soomin Park: 0000-0001-6787-2098

Graham R. Fleming: 0000-0003-0847-1838

Author Contributions

[▽]S.P. and A.L.F. contributed equally to this work.

Notes

The authors declare no competing financial interest.

■ ACKNOWLEDGMENTS

This work was supported by U.S. Department of Energy, Office of Science, Basic Energy Sciences, Chemical Sciences, Geosciences, and Biosciences Division under Field Work Proposal 449B. K.K.N. is an investigator of the Howard Hughes Medical Institute. We thank Dr. Doran I. G. Bennett for helpful discussions and Drs. Liang Guo and Myeongkee Park for technical support.

■ REFERENCES

(1) Krause, G. H.; Weis, E. *Photosynth. Res.* **1984**, *5*, 139−157.
(2) Tripathy, B. C.; Oelmüller, R. *Plant Signaling Behav.* **2012**, *7* (12), 1621−1633.
(3) Müller, P.; Li, X.-P.; Niyogi, K. K. *Plant Physiol.* **2001**, *125* (4), 1558−1566.
(4) Pinnola, A.; Bassi, R. *Biochem. Soc. Trans.* **2018**, *46*, 467−482.
(5) Demmig-Adams, B.; Cohu, C. M.; Muller, O.; Adams, W. W., III *Photosynth. Res.* **2012**, *113*, 75−88.
(6) Zaks, J.; Amarnath, K.; Sylak-Glassman, E. J.; Fleming, G. R. *Photosynth. Res.* **2013**, *116*, 389−409.
(7) Jahns, P.; Holzwarth, A. R. *Biochim. Biophys. Acta, Bioenerg.* **2012**, *1817*, 182−193.
(8) Demmig-Adams, B. *Biochim. Biophys. Acta, Bioenerg.* **1990**, *1020*, 1−24.
(9) Niyogi, K. K.; Grossman, A. R.; Björkman, O. *Plant Cell* **1998**, *10*, 1121−1134.
(10) Demmig-Adams, B.; Adams, W. W. *Environ. Exp. Bot.* **2018**, *154*, 1−3.
(11) Young, A. J.; Frank, H. A. *J. Photochem. Photobiol., B* **1996**, *36*, 3−15.
(12) van Amerongen, H.; van Grondelle, R. *J. Phys. Chem. B* **2001**, *105*, 604−617.
(13) Kloz, M.; Pillai, S.; Kodis, G.; Gust, D.; Moore, T. A.; Moore, A. L.; van Grondelle, R.; Kennis, J. T. M. *J. Am. Chem. Soc.* **2011**, *133*, 7007−7015.
(14) Holt, N. E.; Zigmantas, D.; Valkunas, L.; Li, X.-P.; Niyogi, K. K.; Fleming, G. R. *Science* **2005**, *307*, 433−436.
(15) Avenson, T. J.; Ahn, T. K.; Zigmantas, D.; Niyogi, K. K.; Li, Z.; Ballottari, M.; Bassi, R.; Fleming, G. R. *J. Biol. Chem.* **2008**, *283* (6), 3550−3558.
(16) Ahn, T. K.; Avenson, T. J.; Ballottari, M.; Cheng, Y.-C.; Niyogi, K. K.; Bassi, R.; Fleming, G. R. *Science* **2008**, *320*, 794−797.
(17) Park, S.; Fischer, A. L.; Li, Z.; Bassi, R.; Niyogi, K. K.; Fleming, G. R. *J. Phys. Chem. Lett.* **2017**, *8* (22), 5548−5554.
(18) Ma, Y.-Z.; Holt, N. E.; Li, X.-P.; Niyogi, K. K.; Fleming, G. R. *Proc. Natl. Acad. Sci. U. S. A.* **2003**, *100* (8), 4377−4382.
(19) Bode, S.; Quentmeier, C. C.; Liao, P.-N.; Hafi, N.; Barros, T.; Wilk, L.; Bittner, F.; Walla, P. J. *Proc. Natl. Acad. Sci. U. S. A.* **2009**, *106* (30), 12311−12316.
(20) Holleboom, C.-P.; Walla, P. J. *Photosynth. Res.* **2014**, *119*, 215−221.
(21) Liao, P.-N.; Holleboom, C.-P.; Wilk, L.; Kühlbrandt, W.; Walla, P. J. *J. Phys. Chem. B* **2010**, *114*, 15650−15655.
(22) Liao, P.-N.; Pillai, S.; Gust, D.; Moore, T. A.; Moore, A. L.; Walla, P. J. *J. Phys. Chem. A* **2011**, *115*, 4082−4091.
(23) Billsten, H. H.; Pan, J.; Sinha, S.; Pascher, T.; Sundström, V.; Polívka, T. *J. Phys. Chem. A* **2005**, *109*, 6852−6859.
(24) Polívka, T.; Sundström, V. *Chem. Rev.* **2004**, *104*, 2021−2071.
(25) Polívka, T.; Herek, J. L.; Zigmantas, D.; Åkerlund, H.-E.; Sundström, V. *Proc. Natl. Acad. Sci. U. S. A.* **1999**, *96*, 4914−4917.

DOI: 10.1021/jacs.8b04844
J. Am. Chem. Soc. 2018, 140, 11965−11973

(26) Li, Z.; Ahn, T. K.; Avenson, T. J.; Ballottari, M.; Cruz, J. A.; Kramer, D. M.; Bassi, R.; Fleming, G. R.; Keasling, J. D.; Niyogi, K. K. *Plant Cell* **2009**, *21*, 1798−1812.
(27) Ruban, A. V.; Berera, R.; Ilioaia, C.; van Stokkum, I. H. M.; Kennis, J. T. M.; Pascal, A. A.; van Amerongen, H.; Robert, B.; Horton, P.; van Grondelle, R. *Nature* **2007**, *450*, 575−578.
(28) Correa-Galvis, V.; Poschmann, G.; Melzer, M.; Stühler, K.; Jahns, P. *Nat. Plants* **2016**, *2*, 15225.
(29) Zaks, J.; Amarnath, K.; Kramer, D. M.; Niyogi, K. K.; Fleming, G. R. *Proc. Natl. Acad. Sci. U. S. A.* **2012**, *109* (39), 15757−15762.
(30) Walla, P. J.; Linden, P. A.; Ohta, K.; Fleming, G. R. *J. Phys. Chem. A* **2002**, *106*, 1909−1916.
(31) Gilmore, A. M.; Shinkarev, V. P.; Hazlett, T. L.; Govindjee. *Biochemistry* **1998**, *37* (39), 13582−13593.
(32) Leuenberger, M.; Morris, J. M.; Chan, A. M.; Leonelli, L.; Niyogi, K. K.; Fleming, G. R. *Proc. Natl. Acad. Sci. U. S. A.* **2017**, *114* (33), E7009−E7017.
(33) Sylak-Glassman, E. J.; Malnoë, A.; De Re, E.; Brooks, M. D.; Fischer, A. L.; Niyogi, K. K.; Fleming, G. R. *Proc. Natl. Acad. Sci. U. S. A.* **2014**, *111* (49), 17498−17503.
(34) Sylak-Glassman, E. J.; Zaks, J.; Amarnath, K.; Leuenberger, M.; Fleming, G. R. *Photosynth. Res.* **2016**, *127*, 69−76.
(35) Schansker, G.; Tóth, S. Z.; Strasser, R. J. *Biochim. Biophys. Acta, Bioenerg.* **2006**, *1757*, 787−797.
(36) Gradinaru, C. C.; van Stokkum, I. H. M.; Pascal, A. A.; van Grondelle, R.; van Amerongen, H. *J. Phys. Chem. B* **2000**, *104*, 9330−9342.
(37) Polívka, T.; Zigmantas, D.; Sundström, V.; Formaggio, E.; Cinque, G.; Bassi, R. *Biochemistry* **2002**, *41*, 439−450.
(38) Barzda, V.; Gulbinas, V.; Kananavicius, R.; Cervinskas, V.; van Amerongen, H.; van Grondelle, R.; Valkunas, L. *Biophys. J.* **2001**, *80*, 2409−2421.
(39) Bennett, D. I. G.; Fleming, G. R.; Amarnath, K. *Proc. Natl. Acad. Sci. U. S. A.*, in press.
(40) Dall'Osto, L.; Cazzaniga, S.; Bressan, M.; Palecèk, D.; Žídek, K.; Niyogi, K. K.; Fleming, G. R.; Zigmantas, D.; Bassi, R. *Nat. Plants* **2017**, *3*, 17033.
(41) Külheim, C.; Agren, J.; Jansson, S. *Science* **2002**, *297*, 91−93.
(42) Kromdijk, J.; Glowacka, K.; Leonelli, L.; Gabilly, S. T.; Iwai, M.; Niyogi, K. K.; Long, S. P. *Science* **2016**, *354* (6314), 857−862.
(43) Hontani, Y.; Kloz, M.; Polívka, T.; Shukla, M. K.; Sobotka, R.; Kennis, J. T. M. *J. Phys. Chem. Lett.* **2018**, *9*, 1788−1792.
(44) Adams, W. W., III; Demmig-Adams, B.; Winter, K. *Plant Physiol.* **1990**, *92*, 302−309.
(45) Bilger, W.; Björkman, O. *Photosynth. Res.* **1990**, *25*, 173−185.
(46) Li, X.-P.; Björkman, O.; Shih, C.; Grossman, A. R.; Rosenquist, M.; Jansson, S.; Niyogi, K. K. *Nature* **2000**, *403*, 391−395.
(47) Li, X.-P.; Müller-Moulé, P.; Gilmore, A. M.; Niyogi, K. K. *Proc. Natl. Acad. Sci. U. S. A.* **2002**, *99* (23), 15222−15227.
(48) van Oort, B.; Roy, L. M.; Xu, P.; Lu, Y.; Karcher, D.; Bock, R.; Croce, R. *J. Phys. Chem. Lett.* **2018**, *9*, 346−352.
(49) Chmeliov, J.; Bricker, W. P.; Lo, C.; Jouin, E.; Valkunas, L.; Ruban, A. V.; Duffy, C. D. P. *Phys. Chem. Chem. Phys.* **2015**, *17*, 15857−15867.
(50) Duffy, C. D. P.; Chmeliov, J.; Macernis, M.; Sulskus, J.; Valkunas, L.; Ruban, A. V. *J. Phys. Chem. B* **2013**, *117*, 10974−10986.
(51) Moya, I.; Silvestri, M.; Vallon, O.; Cinque, G.; Bassi, R. *Biochemistry* **2001**, *40*, 12552−12561.
(52) Fox, K. F.; Ünlü, C.; Balevičius, V.; Ramdour, B. N.; Kern, C.; Pan, X.; Li, M.; van Amerongen, H.; Duffy, C. D. P. *Biochim. Biophys. Acta, Bioenerg.* **2018**, *1859*, 471−481.

DOI: 10.1021/jacs.8b04844
J. Am. Chem. Soc. 2018, 140, 11965−11973